

REVIEWS ESSD-2022-163, Lizotte et al., Preprint

Nunataryuk field campaigns: Understanding the origin and fate of terrestrial organic matter in the coastal waters of the Mackenzie Delta region

We thank the two anonymous reviewers who took the time to write thoughtful and very constructive comments on the first version of the paper. Below we address each comment and bring the necessary changes to the text.

ESSD-2022-163, Referee #1 comments, 23 Sept 2022

RC1The manuscript presents information pertaining to the amount and quality of OM supplied to the Arctic Ocean and focuses on the fate of terrestrially-derived OM from coastal erosion, river runoff and potential permafrost contributions. The authors provide a summary and data from four field expeditions in the Mackenzie River Delta collected over 2019.

I find little to criticise with this paper. It is well structured and easy to follow with well-annotated figures. The table summary at the end is clear, however the Pangaea-download appears to be locked and under moratorium until November. As such, it is unclear how to test access to the datasets shown here. The table summary and information at the end of the manuscript are clear and helpful. I appreciate the available code to reproduce the figures. Congratulations to the authors for their work, especially given the breadth of the data provided here.

1-My main question is surrounding authorships. Provided close partnerships with community members noted throughout the manuscript and acknowledgements, wouldn't far more inclusion of community members involved in the work not be suitable? Were none of the community members essential in the work conducted?

Author reply: We wholeheartedly agree with the anonymous referee. The appropriate recognition of all team members is crucial, including the contributions of community members. That is why David Obie James Anikina and Charlotte Irish (Tuktoyaktuk Community Corporation, Tuktoyaktuk, Canada), Miles Dillon (Inuvik Hunters and Trappers Committee, Inuvik, Canada) and Thomas J. Gordon (Aklavik Hunters and Trappers Committee, Aklavik, Canada) are all contributing co-authors on this paper recognizing their essential role in the success of the research (please see Author Contributions section, line 559 and onwards). Finally, we also recognize the contributions of specific community members from Aklavik, Inuvik and Tuktoyaktuk in the acknowledgement section: Michelle Gruben, Raymond Etagiak, Sammy Gruben Jr., James Keevik, Rachael Keevik, Charles Pokiak, Kendyce Cockney, Dave Mcleod, Shauna Charlie, JD Storr, Douglas Esagok, Jimmy Nuilak Kalinek, Cassandra Paul, and Davonna Kasook.

2-Throughout, little information is provided on the error and uncertainties associated with the instruments and methodologies used. Can this be more clearly highlighted in the text, or state that it is in the associated data files (assuming it is?)

Author reply: We amended the text in several sections of the manuscript to include information about error/precision/uncertainties of the methods and instruments used when missing. Please see added details **in bold** below:

- Section 4.1 Physical and optical data.

Vertical profiles of underwater conductivity (Figs. 5 and 6A), conservative temperature (Fig. 6B) and depth (CTD) were measured at each site by deploying and immediately recovering using two RBR sensors: a Maestro model (depth rating of 100 m) during Leg 1, and a Concerto model (depth rating of 50 m) during Legs 2, 3 and 4. The sensors, chosen for their high vertical resolution **and accuracy (see below)**, were deployed either alone (Leg 1) or fitted to a frame together with various optical sensors (Legs 2, 3 and 4). As recommended by the instrument manufacturer, the conductivity cell was placed more than 15 cm away from any other structure. Both sensors were factory-calibrated prior to the expeditions and deployed either through the ice (Leg 1) or directly into the water column (Legs 2, 3 and 4) from helicopters or boats. **The manufacturer gives an initial accuracy of +/- 0.003 mS cm⁻¹ for the conductivity, +/- 0.002 °C for the temperature and +/- 0.05 % of sensors maximum depth (i.e., 0.05 m for the Maestro model and 0.025 m for the Concerto model that have been used), see <https://docs.rbr-global.com/support/sensors/sensors-and-specification>.**

- Section 4.1.2. Absorption coefficients for **colored chromophoric** dissolved organic matter

Water samples for the determination of absorption coefficients for **colored chromophoric** dissolved organic matter (a_{CDOM}) were filtered within 12h of water collection using 0.2 μm GHP filters (Acrodisc Inc.) pre-rinsed with 200 ml of Milli-Q water. Filtered samples were then pumped into the sample cell of an UltraPath liquid waveguide system (World Precision Instruments, Inc.) using a peristaltic pump, and the absorption coefficient was measured over the wavelengths ranging from 200 to 722 nm (see Bricaud et al., 2010 and further modifications in Matsuoka et al. (2012) for the complete analytical procedures). **For most samples a 10 cm cell was used. For a limited number of cases, when low signal in the spectral domain was observed (mostly waters further offshore), a 200 cm cell was used instead. For a limited number of cases, when low signal in the spectral domain was observed (mostly waters further offshore), a 200 cm cell was used instead. Due to a complete absorption of light in the UV-range even when using the 10 cm pathlength, measurements from 200 to 280 nm were masked. To ensure quality of the rest of the data, individual spectra were carefully checked for potential saturation, following recommendations by Lefering et al. (2017). A threshold of 1.2 absorbance unit (AU) was used, and only the data lower than the AU was included in this study.** Measurements and sample processing were conducted following the protocol *Ocean Optics and Biogeochemistry* from the International Ocean Color Coordinating Group (IOCCG Protocol Series, 2018). **Uncertainty for most of the measurements was less than five percent (determined using replicate scans).**

- Section 4.1.3. Dissolved organic carbon

To determine concentrations of dissolved organic carbon (DOC), 20-25 mL of water was collected into a sterile 30-mL syringe void of a rubber piston. The water was then filtered through a pre-cleaned (acid-washed and MilliQ water rinsed) filter-holder containing a 25 mm Whatman GF/F (0.7 μm), and acidified with 20 μL Suprapur HCl (10 M) on the same day of sampling. DOC samples were stored and kept at 4 °C in the dark during transport until further analysis. Concentration of DOC was measured using high-temperature catalytic oxidation (TOC-VCPH, Shimadzu) at the Alfred-Wegener-Institute (AWI) Potsdam, Germany. Blanks (Milli-Q water) and certified reference standards (Battle-02, Mauri-09 or Super-05 from the National Laboratory for Environmental Testing, Canada) were measured for quality control. **The uncertainty for DOC was derived from the deviation of the DOC standards that were used during the analysis. DOC standards with concentrations of 1.24, 4.64, 7.31, 25.0, and 103,4 mg L⁻¹ were used. The uncertainty is the average percentage deviation from the measurement and the certified value. The results of standards provided an accuracy better than ± 5 %.** Seasonal trends in DOC reveal a range of concentrations from a minimum of 1.7 mg L⁻¹ to a maximum of 8.8 mg L⁻¹ (Fig. 6E and Table 2) with the lowest median concentrations of DOC observed during summer (Leg 3).

- Section 4.1.5. Suspended particulate matter

Water samples for the determination of suspended particulate matter (SPM), as well as concentrations of total particulate carbon and nitrogen (TPC and TPN, respectively), were filtered through a glass filtration unit on pre-weighed, pre-combusted blank Whatman GF/F (0.7 μm) 47 mm filters. After filtering volumes of water ranging from 150 to 1000 mL, the filters were transferred to labeled petri dishes (previously acid-washed and MilliQ water rinsed) and placed in the oven to dry overnight at 60 °C before being vacuum sealed for storage and shipment. Analysis for SPM, TPC and TPN was conducted at Laval University (Quebec City) at the end of 2019. Samples were weighed three times each with a Mettler Toledo microscale after a final overnight drying at 60 °C to remove any leftover moisture. Values for SPM were obtained by subtracting the initial weight of blank filters from the final weight of the particulate matter laden filter. Due to the presence of large amounts of matter, subsections of the filters were **randomly** taken with a specialized punching tool. Two punched replicates were placed into tin capsules and processed in a Perkin Elmer elemental analyzer (PE 2400 Series-II CHNS/O Analyzer). **Considering that the average coefficient of variation for every pair of random punches was only 3 % for carbon measurements and 7 % for nitrogen measurements,** concentrations of TPC and TPN were obtained by extrapolating data from the punched subsection diameter to full filter diameter, assuming uniformity of particulate matter on the filter. As shown in Fig. 6G, Leg 1 was characterized by near zero SPM concentrations, while Legs 2, 3 and 4 exhibited higher median values around 50 μg SPM mL⁻¹.

- Section 4.1.6. Particulate organic matter

Water samples for the determination of particulate organic carbon (POC) and nitrogen (PON) were filtered through a glass filtration unit on pre-combusted Whatman GF/F (0.7 μm) 47 mm filters with filtration volumes ranging from 250 to 1600 mL. Resulting filters were then placed into petri dishes (previously acid-washed and MilliQ water rinsed) and transferred to the oven at 60 °C to dry overnight before being vacuum sealed for storage and shipment to Laval University (Quebec City) for analysis. In order to solely preserve the organic fraction of the particulate matter, all samples were acidified with pure HCl (37% w/w) placed into a container at the bottom of a dessicator. Following a 72 hr exposure to HCl vapors, the filters were exposed to sodium hydroxide (NaOH) during 72 h to neutralize the samples. Using a punching tool, the filters were sectioned into two sub-samples that were individually wrapped in tin capsules prior to analysis. The 47 mm filters had to be sub-sectioned as they did not fit fully into the analysis capsules. These capsules were processed in a Perkin Elmer elemental analyzer (PE 2400 Series-II CHNS/O Analyzer, **accuracy ≤ 0.3 % and precision ≤ 0.2 %**) to obtain masses of carbon and nitrogen. A cross-product calculation was used to extrapolate POC and PON concentrations from the punched subsection diameter to full filter diameter. As shown in Fig. 6H, Leg 1 was characterized by near zero POC concentrations, while Legs 2, 3 and 4 exhibited slightly higher median values around 1 $\mu\text{g POC mL}^{-1}$. Basic information related to PON values can be found in Table 2.

-Section 4.1.7 Particulate absorption

Coefficients for the absorption of light by particles were obtained within ca. 12 h of water collection using a spectrophotometer (Cary 100, Agilent Technologies Inc.) equipped with a small (60 cm) integrating sphere. Samples were prepared by filtering volumes of water (from approximately 20 to 500 mL, depending on turbidity) onto 25 mm Whatman GF/F filters, with a minimum of 5 stations measured in duplicate or triplicate every day. To minimize biases due to backscattering by particles retained on the sample filter, the transmittance and reflectance were measured from 350 to 800 nm at 1 nm increments (so-called T-R method; Tassan and Ferrari, 1995; 2002). A recent study demonstrated that the T-R method is particularly useful for turbid waters (Stramski et al. 2015; IOCCG Protocol Series 2018), such as those found in the Mackenzie River and Delta. The derived absorbance was then converted into absorption coefficients ($a_p(\lambda)$, m^{-1}) by taking into account the volume of water filtered and the clearance area of the filter. The final $a_p(\lambda)$ was determined by applying a beta factor (Mitchell et al., 2003) specific to our instrument set-up (Tassan and Ferrari, 2003), allowing the extrapolation of the absorption of particles concentrated on the filter to what would be in suspension. **Throughout the legs, the median uncertainty for the final $a_p(\lambda)$ determination was lower than 3 %.**

- Section 4.1.8 Radiometric data

In order to evaluate atmospheric correction algorithms and develop/evaluate algorithms for deriving in-water constituents from reflectance, surface irradiance (E_s^{0+}) along with

vertical profiles of downwelling irradiance (E_d) and upwelling radiance (L_u) of the water were measured during boat sampling of Legs 2, 3 and 4 using a Compact-Optical Profiling System (C-OPS, from Biospherical instruments, Inc., see a complete description of the system in Morrow et al. (2010)). Measurements of C-OPS radiometric light levels could not be acquired in the waters of Shallow Bay and Mackenzie Bay (western sector) during Leg 2 due to the lack of space aboard the helicopter, as well as for safety reasons associated with free cables outside the cockpit of the hovering aircraft. The C-OPS system was composed of a set of highly sensitive radiometers, which acquire radiometric measurements in water and in air. In order to correct in-water E_d and L_u for changes in the incident light field during L_u profiling, above-surface downwelling incident irradiance (E_s^{0+}) was measured at about two meters above sea level and above any boat structure during the time of profiling (Zibordi et al., 2019). From the E_d and L_u profiles, apparent optical properties (AOP), such as the diffuse attenuation coefficient or the remote-sensing reflectance, were computed (Bélanger et al., 2017). **The C-OPS measurement accuracy has been fully characterized in Morrow et al. (2010), where the C-OPS underwater irradiance integrated error is found to be less than 2.5 % (less than 1.5 % for the in air irradiance), and where the C-OPS data have also been compared to other well established sensor data. The reported average unbiased percentage difference (UDP) ranges from -2.2 % to 1.8 % (depending on the radiometric parameter under consideration and on water type), which falls within calibration uncertainties. The UDP is defined as $UDP = 200 \times (S_{test} - S_{ref}) / (S_{test} + S_{ref})$, where S_{ref} are the reference sensor data and S_{test} are the tested sensor data. A more recent and complete instrument characterization (Hooker et al., 2018, as well as a personal communication from Biospherical Instruments, Inc.) give very similar figures (see, for example, their section 8.6 and their table 16). The uncertainty on the remote sensing reflectance, which is the ratio of the water-leaving radiance and the downwelling irradiance just above the sea-surface, could be estimated, to a first approximation, with a quadrature combination. An average uncertainty of 2.5 % in both radiance and irradiance yields to an uncertainty on the remote sensing reflectance of 3.54 %. This uncertainty, however, does not include the uncertainty related to the estimation of the water-leaving radiance from the upward radiance profile.**

- Section 4.1.9 Inherent optical properties

Following comments by the second reviewer, this entire section was reworded to reflect the unfinished status of this part of the dataset:

~~4.1.9 Inherent optical properties~~

~~To measure inherent optical properties (IOP) in the water column, an optical package was deployed during all four legs of the expedition. During Leg 1, the optical package included a very sensitive depth sensor (RBR model Virtuoso, accurate to 0.01 m), a particle size distribution and concentration meter (Sequoia Scientific, model LISST 100x, sensitive to 0.1 mg L^{-1}), as well as a data logger (Seabird Scientific, model DH4), all fitted in a cylindrical metallic frame that was manually lowered through an auger hole in the ice using a tripod and a hoisting system. During Legs 2, 3 and 4, the optical package included a different secondary~~

~~CTD (RBR Concerto, see section 4.1 for its specifications), the same particle size distribution and concentration meter and data logger, 2 back scattering meters (a HydroScat 2 from HobiLabs, accurate to 1×10^{-4} to $1 \times 10^5 \text{ m}^{-1}$) and a BB3 from Seabird Scientific, accurate to 0.003 m^{-1}), and a fluorescence meter (model FLBBCD from Seabird Scientific, accurate to $0.015 \mu\text{g L}^{-1}$ for the chlorophyll a pigment and to 0.28 ppb for the CDOM). All the sensors were factory calibrated prior to the expedition. The cylindrical frame was lowered at sea using a drill-operated winch during helicopter hovering flights, or using a motorized pulley with a davit when sampling from small fishing boats. In both cases, an electro-mechanical cable allowed for real-time data acquisition and minimal quality control. The instrumentation descent rate was very slow (ca. 0.05 - 0.20 m s^{-1}) to allow for a maximal resolution of the strong vertical gradients characteristic of several of the stations sampled. See Table 2 for details on availability of data.~~

4.1.9. Other optical parameters

A so-called optical frame was also deployed during the boat sampling of the Legs 2, 3 and 4. This frame was equipped with: a BB3 from SeaBird Scientific, a FLBBCD from Seabird Scientific, a HydroScat-2 from HobiLabs, an AC-9 (with a 10 cm pathlength) from SeaBird Scientific, as well as a LISST-100X (sometimes fitted with a path reduction module, in very turbid waters) from Sequoia Scientific. These sensors allow to retrieve profiles of the backscattering coefficients at six wavelengths, the concentration of Chl-a and of CDOM, the absorption coefficients at nine wavelengths, the beam attenuation at nine wavelengths, as well as particle volume and size distribution between 1.25 and 250 microns. These data have not yet been fully processed and will be published at a later time (see Appendix D for further information on the processing of light absorption (a) and scattering (b) coefficients).

- Section 4.2 Nutrients

Samples for the determination of nitrate, nitrite, phosphate and silicate concentrations (Fig. 9) were obtained from water filtered through consecutive $0.7 \mu\text{m}$ Whatman GF/F filters and $0.2 \mu\text{m}$ cellulose acetate membranes. Filtrates were collected in duplicate sets of sterile 20-mL polyethylene vials, with one set being immediately stored at -20°C , while a second set was poisoned with $100 \mu\text{L}$ of mercury chloride (60 mg L^{-1}) and subsequently stored in the dark at 4°C until analysis. Nutrient concentrations were determined at Laval University (Quebec City) using an automated colorimetric procedure described in Downes (1978) and Grasshoff (1999). **The detection limits were 0.03, 0.02 and 0.05 mmol L^{-1} for $\text{NO}_3^- + \text{NO}_2^-$, PO_4^{3-} and Si(OH)_4 , respectively. The precision of triplicates over the observed range of concentrations was similar to, or better than, these detection limits.**

- Section 4.3.1 Phytoplankton pigments

A full list of accessory pigments analyzed in this study is available in Table 2. Median concentrations of Chl *a* over the study region were at their lowest during winter (Leg 1, Fig. 10), while the greatest interquartile range and highest median concentrations were observed throughout the summer stations (Leg 3, Fig. 10). Despite their seasonal variability, concentrations of Chl *a* were proportionally dominant over all other photosynthetic and non-photosynthetic pigments analyzed across the sampled stations (see example for three selected stations in Fig. 11). **At the time samples were analyzed, analysis precision was 0.6 % (Chl *a*) and 2.3 % (all other pigments).**

- Section 4.3.2 Bacterioplankton abundance and diversity

Samples for the determination of bacterial abundance were prepared immediately at the Aurora Research Institute (Inuvik) upon reception of the water. A volume of 1.5 mL of water was pipetted into a 2 mL Nunc Cryotube containing 15 µl of 25% glutaraldehyde. The Cryotubes were vortexed for 5 s, allowed to sit at room temperature for 10 min, then stored in cryoboxes at -80°C before analysis by flow cytometry with SYBR™ Green I (ThermoFisher Scientific) (Gasol and Del Giorgio, 2000) at the **Laboratoire d'Océanographie Microbienne, Banyuls/mer, France. The mean coefficient of variation for this quantification was below to 5 % (n = 3).** Median concentrations of bacterial cells (Fig. 10B) were lowest during Leg 1 and highest during the summer months (Legs 2 and 3).

DNA extraction was performed using Qiagen PowerSoil kits following the instructions provided by the manufacturer and DNA extracts were quantified on a Qubit fluorometer (**the mean coefficient of variation for such quantification was about 30 %**). Extracts were sent to Integrated Microbiome Resource (U. Dalhousie, Halifax, Canada) where library preparation, multiplexing, and sequencing were performed **for bacteria**. The sequencing targeted the V4-V5 regions of the 16S rRNA gene using the 515FB (5'-GTGYCAGCMGCCGCGTAA-3') and 926R (5'-CCGYCAATYMTTTRAGTTT-3') primer sets (Parada et al., 2016; Walters et al., 2016). Sequencing was performed on an Illumina MiSeq platform, and sequences were then analyzed using the dada2 pipeline v1.16 (Callahan et al., 2016) in R v4.1.2 (R Core Team, 2021) and R-Studio (v1.2.1335). Taxonomy assignment was performed up to the Genus level with SILVA reference database v138 (Quast et al., 2013). Details on Amplicon Sequence Variants (ASVs) of bacterial communities are given in Table 2.

- Section 4.3.3 Fungal abundance and diversity

Following DNA extraction (see above), fungal abundance was evaluated by real-time quantitative PCR (qPCR) using the primer set FungiQuant-F: 5'-GGRAAACTCCACCAGGTCCAG-3' and FungiQuant-R: 5'-GSWCTATCCCCAKCACGA-3' (Liu et al., 2012) and following the protocol described in Maza-Márquez et al. (2020). **The mean coefficient of variation for such quantification was about 25 % (n = 3).**

- Section 4.3.4 Microbial respiration

Microbial respiration rates (see metadata in Table 2) were derived from continuous dissolved oxygen (O₂) measurements using a SensorDish Reader (SDR; Presens, Germany) optical sensing system equipped with 24 glass vials of 5 mL containing non-invasive O₂ sensors (OxoDish). The sensor vials were top filled with sample water then sealed without headspace or bubbles and inserted into the SDR plate. The entire setup was placed in an incubator at a constant temperature of 10 °C. Dissolved O₂ concentrations were derived from 10 minute averages of quenched fluorescence measurements taken every minute over a period of 10 hours. Linear regression analysis was performed on the dissolved O₂ concentration data from each vial to determine microbial respiration (μmol O₂ L⁻¹ h⁻¹). **The mean coefficient of variation for this measurement was about 20 % (n = 3).**

- Section 4.4.1 Sediment and pore water

Cations were analyzed with Agilent 8800 ICP-QQQ-MS while DOC analysis was conducted on a Shimadzu Total Organic Carbon Analyzer TOC-VCPH (**Neweshy et al., 2022**). Sand sulfides were analyzed using a Horiba Scientific Aqualog and analysis of anions will be conducted by Dionex Integrion HPIC (High Performance Ion Chromatography) (Couture et al., 2016). To ensure instrumental accuracy, certified reference materials were used when available. **The accuracy and precision of each method was evaluated with the results from these analyses. When no certified reference materials were available, control samples were prepared by another scientist to ensure that no systematic errors are applied to samples and that the calibration curves are accurate. When control samples were used, measurements were taken 10 times and a variation of 10% was accepted.**

The sediment cores were sliced every 1 cm. The subsamples were placed in Falcon cups and kept frozen until treatment. The samples were then freeze-dried and homogenized with an agate pestle and mortar. Ground, freeze-dried sediment was mineralized using ultra-pure nitric and hydrochloric acids using a microwave (MARS5 Microwave in EasyPrep vessels). Results were validated against MESS-4 certified reference material (National Research Council Canada). The mineralisation protocol used is based on Ma et al. (2019) with further modifications detailed in Bossé-Demers, T. *et al.* (in prep.).

Major (Fe, Ca, Na, Mg, Mn and K) and rare-earth elements (REE) in the sediment were analyzed using a Thermo Scientific iCAP 7400 ICP-OES and an Agilent 8800 ICP-QQQ-MS, respectively.

For cations pore water analysis, SLRS-6 from the National Research Council Canada (Ottawa, Canada) certified reference material was used to validate the method (n = 3). The values were always within 12% of certified values. The precision, expressed as the coefficient of variation of replicates analysis was under 10% for most analytes.

For cation sediment analysis, MESS-4 from the National Research Council Canada (Ottawa, Canada) certified reference material was used to validate the method (n = 9). The values were always within 8% of certified values. The precision, expressed as the coefficient of variation of replicates analysis, was under 10% for all analytes.

~~The sediment cores were sliced every 1 cm. The subsamples were placed in Falcon cups and kept frozen until treatment. The samples were then freeze-dried and homogenized with an agate pestle and mortar. Ground, freeze-dried sediment was mineralized using ultra-pure nitric and hydrochloric acids using a microwave (MARS5 Microwave in EasyPrep vessels). Results were validated against MESS-4 certified reference material (National Research Council Canada). The mineralisation protocol used is based on Ma et al. (2019) with further modifications detailed in Bossé-Demers, T. et al. (in prep.). Major (Fe, Ca, Na, Mg, Mn and K) and rare-earth elements (REE) in the sediment were analyzed using a Thermo Scientific iCAP 7400 ICP-OES and an Agilent 8800 ICP-QQQ-MS, respectively.~~

3-109: I am not sure if privileged is the correct word in this sentence.

Author reply: We have changed the wording of the phrase to take into account the referee's comment

Original version: *"With the presence of consolidated sea ice in the coastal waters of the Beaufort Sea during Leg 1 (Fig. 4), helicopter flights out of Inuvik to the western sector of the coastal waters (Shallow and Mackenzie bays) were privileged due to the large distance separating 110 the sampling area and the nearest community (Aklavik) as well as the impossibility to set up camp near the coast."*

Modified version: *"With the presence of consolidated sea ice in the coastal waters of the Beaufort Sea during Leg 1 (Fig. 4), helicopter flights **were carried** out of Inuvik to the western sector of the coastal waters (Shallow and Mackenzie bays) due to the large distance separating 110 the sampling area and the nearest community (Aklavik) as well as the impossibility to set up camp near the coast."*

4-140: So to be clear, these were used to profile the water column at each site and not left in-situ at all? Can you just make this more clear earlier as I wasn't sure on first quick read until later on.

Author reply: We agree with the referee that this could be made clearer. We made modifications to the below phrase that we believe brings that clarity.

Original version: “*Vertical profiles of underwater conductivity (Figs. 5 and 6A), conservative temperature (Fig. 6B) and depth (CTD) were measured using two RBR sensors: a Maestro model (depth rating of 100 m) during Leg 1, and a Concerto model (depth rating of...*”

Modified version: “*Vertical profiles of underwater conductivity (Figs. 5 and 6A), conservative temperature (Fig. 6B) and depth (CTD) were measured **at each site by deploying and immediately recovering** two RBR sensors: a Maestro model (depth rating of 100 m) during Leg 1, and a Concerto model (depth rating of...*”

5-Figure legends and text could be made clearer and larger in many of the figures. Maybe I'm old.

Author reply: The format of the legend is prescribed by the latex template provided by ESSD. However, in order to help with this we have increased the base font size from 10 pt to 12 pt.

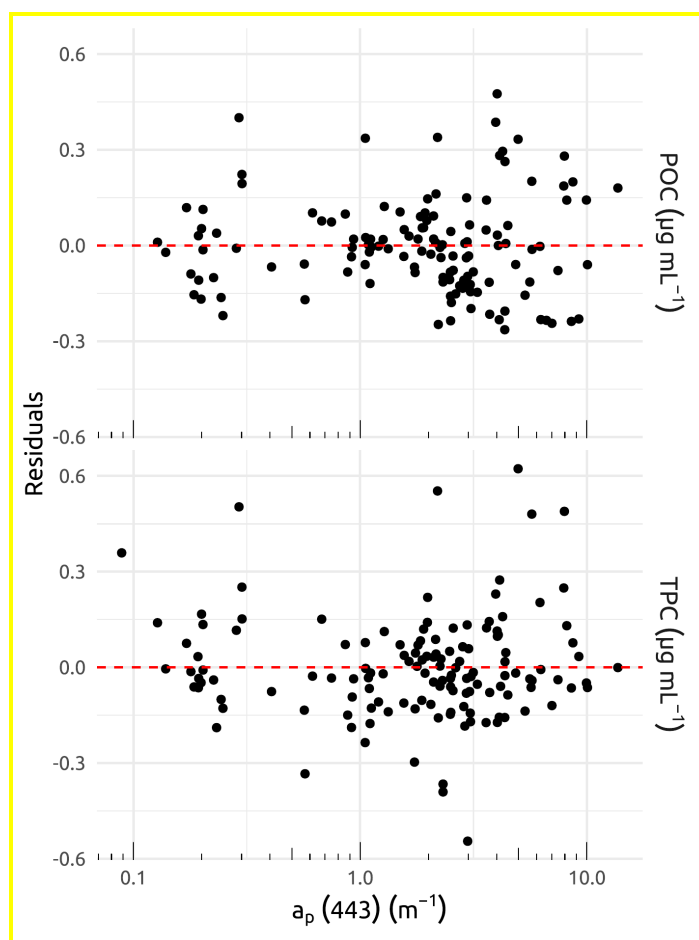
6-221-223 "Concentrations of TPC and TPN on filter subsamples required extrapolation assuming uniformity of particulate matter on the filter". Do you have any estimates for the actual variability in TPC/ TPN across the filter, i.e. multiple subsection punches from the same filter?

Author reply: We added information on variability across filter punches. See modifications in **bold**.

Due to the presence of large amounts of matter, subsections of the filters were **randomly** taken with a specialized punching tool. Two punched replicates were placed into tin capsules and processed in a Perkin Elmer elemental analyzer (PE 2400 Series-II CHNS/O Analyzer). **Considering that the average coefficient of variation for every pair of random punches was only 3 % for carbon measurements and 7 % for nitrogen measurements,** concentrations of TPC and TPN were obtained by extrapolating data from the punched subsection diameter to full filter diameter, assuming uniformity of particulate matter on the filter.

7-245 Leg 1 certainly shows more scatter at the lower end of the POC, TPC and ap(443). Is this within the instrumental measurement error range? Do we have higher uncertainty in the TPC measurements? Whilst I agree that Leg 1 generally fits within the linear regression shown, a little note of whether this pattern is likely down to instrumental uncertainty, or may suggest something else would be helpful.

Author reply: Because the data is plotted on a log-scale, the scatter is actually not higher at the lower end of POC aP and TPC. According to the plots below (see figure), the residuals seem to be relatively homogeneously spread around the zero line (not necessarily just at the lower end of the plot, but really throughout, for both POC and TPC).



We added the following sentence at the end of figure 7 caption to reflect this:

Figure 7. Linear regressions between particle absorption ($a_p(\lambda)$) at 443 nm and: (A) particulate organic carbon (POC); (B) total particulate carbon (TPC) for the four WP4 Nunataryuk expeditions (Legs 1, 2, 3 and 4) in 2019. Equations and coefficients of determination (R^2) are shown. The blue lines represent the linear regressions, whereas the shaded gray areas show the standard error around the regression lines. **Note that the data are plotted on a log-scale.**

8-Figure 8. Can you please add a description of the units in the figure legend?

Author reply: There is no legend in this figure but we did modify the caption to take into account the referee's comment:

Original caption: Figure 8. Remote sensing reflectance (R_{rs}) spectra measured using the C-OPS between 395 and 865 nm during Legs 2, 3 and 4. Note that R_{rs} spectra were not measured during Leg 1.

Modified caption: Figure 8. Remote sensing reflectance (R_{rs} , **per steradian**) spectra measured using the C-OPS between 395 and 865 nm during Legs 2, 3 and 4. Note that R_{rs} spectra were not measured during Leg 1.

9-Nutrients - uncertainty in concentrations using these colourimetric methods? The lowest limit of detection?

Author reply: The following phrase was added: **The detection limits were 0.03, 0.02 and 0.05 mmol L⁻¹ for NO₃⁻+NO₂⁻, PO₄³⁻ and Si(OH)₄, respectively. The precision of triplicates over the observed range of concentrations was similar to, or better than, these detection limits.**

10-Fig 10. data points excluded were from Leg 2 of Fig 10b correct? Please clarify the legend.

Author reply: We modified the information in the figure caption to make it clearer.

Original caption: Figure 10. Box plots of : (A) Chlorophyll *a* (Chl *a*) concentration (mg m⁻³); and (B) Bacterial abundance (cells mL⁻¹) for the four WP4 Nunataryuk expeditions (Legs 1, 2, 3 and 4) in 2019. Boxes represent the interquartile range (IQR), the horizontal lines show the medians, while the vertical lines show data spread with min/max whiskers. Notice the y-log10 scale. Also note that a few data points below 100K (Leg 2) were excluded from this graphical presentation.

Modified caption: Figure 10. Box plots of : (A) Chlorophyll *a* (Chl *a*) concentration (mg m⁻³); and (B) Bacterial abundance (cells mL⁻¹) for the four WP4 Nunataryuk expeditions (Legs 1, 2, 3 and 4) in 2019. Boxes represent the interquartile range (IQR), the horizontal lines show the medians, while the vertical lines show data spread with min/max whiskers. Notice the y-log10 scale. Also note that a few data points below 100K (Leg 2) were excluded **from panel b**.

11-390 To clarify, these supplemental datasets (e.g. radon, gases) are also available in Juhls et al. 2021?

Author reply: Not all the datasets are currently available in Juhls et al. 2021. Table 2 gives a detailed account of the status of each dataset (available, in progress, on request) as well as information about who to contact (person and email) and the reference DOI when available. Information on the availability of ALL datasets (including radon, gases, etc.) can be found in Table 2.

12-Table 2 - method "spectrofluorometry" is spelt incorrectly.

Author reply: Thank you for seeing this. Corrections have been applied.

ESSD-2022-163, Referee #2 comments, 14 December 2022

General Comments:

1-The manuscript by Lizotte et al. describes a large and unique data set of physical, biological, and biogeochemical properties/variables acquired in the Mackenzie River Delta region in 2019. The data set is directly relevant to our understanding of the origin and fate of terrestrial organic matter during four sequential legs that covered the pre-freshet, freshet, and post-freshet period of 2019. The data itself have already been published (Juhls et al, 2021) and this manuscript provides a description portion of this data set. This is a very valuable data set that represents a major effort by multiple investigators working in a remote area. The collection of such a complete data set across different seasons covering the pre-freshet to late summer is unprecedented (as far as I know) and this is excellent that the data is made available to the greater community. Overall, the manuscript does a good job at describing the field campaigns, the sampling, and the data available. The figures are of high quality and generally clear and self-explanatory.

Author reply: We thank reviewer #2 for the rigorous work conducted and the very high quality revision. The author's response that follows details how we took into account each and every comment made.

2-The manuscript is generally well written, although writing style can be improved in some parts where sentences are a bit wordy, long and convoluted. I suggest spending a little more time on editing and making sure that shorter, more direct sentences are used. This is especially true at the beginning of the manuscript (examples: sentences on Lines 36-41, and Lines 30-32).

Author reply:

The following modifications were brought to lines 36-41:

Original phrase: Gaining greater insight into these processes is crucial as they may lead, among other things, to enhanced emissions of CO₂ or other greenhouse gasses (Semiletov et al., 2013; Vonk et al., 2012; Vonk and Gustafsson, 2013; Tanski et al., 2019) and modifications in the productivity of the primary producers (Kipp 40 et al., 2018) that sustain the marine arctic food web, with unknown impacts on the communities that rely on these food sources (Fritz et al., 2017).

New phrases: Gaining greater insight into these processes is crucial as they may lead to enhanced emissions of CO₂ or other greenhouse gasses (Semiletov et al., 2013; Vonk et al., 2012; Vonk and Gustafsson, 2013; Tanski et al., 2019). Changes in primary production(Kipp 40 et al., 2018) that sustains the marine arctic food web may also arise with unknown impacts on the communities that rely on these food sources (Fritz et al., 2017).

The following modifications were brought to lines 30-32:

Original phrase: While permafrost thaw is ongoing, well-established, and its rate is accelerating (Camill, 2005; Biskaborn et al., 2019), the fate of the newly-mobilized OMT, as it transits from watersheds, to rivers and at the subsurface, into coastal waters of the Arctic Ocean remains poorly understood.

New phrase: While permafrost thaw is ongoing and its rate is accelerating (Camill, 2005; Biskaborn et al., 2019), the fate of the newly-mobilized OMT as it transits from watersheds to rivers and into coastal waters of the Arctic Ocean remains poorly understood.

3-There is also a need for a better balance of details and description between the different sections as this aspect can be uneven in some parts. The manuscript needs to be more balanced throughout in term of the level of details and referencing used to describe the methods and data. Some parts being very detailed (perhaps too detailed) and other being too succinct and without references. The authors should make sure all sections have methods cited and an appropriate level of details. I point out a few places where this is a problem in the “specific comments”.

Author reply: We thank the reviewer for pointing out specific sections where this issue occurs. We have taken every suggestion and made modifications accordingly, please see below. Some of the comments made by both reviewers (#1 and #2) overlapped in this regard (please see answers to comment #2 by reviewer #1) . We believe the modifications we made help to address this issue.

4-It is very evident that different sections were written by different contributors (as expected), but the style could be harmonized a little bit more across the manuscript.

Author reply: We fully appreciate the nature of this comment and do agree that the writing styles of the paper are not fully homogenized. With 45+ co-authors, the task of ensuring total homogeneity would be difficult. We did however respond to each of the specific comments made that address this issue (see below). We thank the reviewer for his rigorous work in finding sections or lines that needed to be refined.

Specific comments:

5-Line 2: I would recommend changing to “in the Mackenzie River Watershed” as permafrost is present in much of the Mackenzie watershed and C released for other parts of the watershed permafrost could also influence the Delta OC dynamics

Author reply: Agreed. “Mackenzie Delta Region” was changed to “Mackenzie River watershed”

6-Figure 1: I would suggest adding the date ranges for each leg in the captions for rapid comparison to the location of points.

Author reply: The dates were added to the caption as follows:

Original caption: Figure 1. Map of the Mackenzie Delta region (Inuvialuit Settlement Region, Northwest Territories, Canada), with bathymetric features (from 0 to > 60 m) of the coastal waters of the southern Beaufort Sea, showing the sampling stations during the four 2019 WP4 Nunataryuk field expeditions (Legs 1, 2, 3 and 4). Note that the Arctic Red River hydrometric station (10LC014) used to retrieve discharge rates (Fig. 3A) is shown.

New caption: Figure 1. Map of the Mackenzie Delta region (Inuvialuit Settlement Region, Northwest Territories, Canada), with bathymetric features (from 0 to > 60 m) of the coastal waters of the southern Beaufort Sea, showing the sampling stations during the four 2019 WP4 Nunataryuk field expeditions (Legs 1, 2, 3 and 4). Note that the Arctic Red River hydrometric station (10LC014) used to retrieve discharge rates (Fig. 3A) is shown. Leg 1 took place from 17 April to 3 May 2019, Leg 2 extended from 14 June to 4 July 2019, Leg 3 took place from 25 July to 8 August 2019, Leg 4 was conducted from 26 August to 9 September 2019.

7-Figure 3: River discharge from the Mackenzie River in 2019 was lower than average I think,...I would recommend adding a statement mentioning it in order to indicate how the 2019 discharge compared to the climatological average (e.g., 2000-2022)...Maybe a plot of the river discharge climatology could be added to Figure 3a.

Author reply: Figure 3A was modified and the 2000-2022 climatological averages (+/-) were added in a gray shaded area. The following information was added in the caption: “...**the gray shaded area in panel A represents mean values (+/- standard deviation) of the climatology from 2000-2022;**...”

Furthermore, the following phrase was added to the text at the end of line 105: **Overall, discharge rates were similar to climatological means (2000-2022) for Leg 1 and Leg 4, but lower compared to the climatology during Leg 2 and Leg 3 (see Fig. 3a).**

8-Figure 4: Mention in caption that there was unconsolidated ice during Leg 2.

Author reply: The following phrase was added at the end of the caption: “Note that there was unconsolidated ice during Leg 2.”

9-Figure 5: Is this showing surface salinity? If not, what was the depth? Please mention in caption. (Because it says profiles in line 139).

Author reply: We acknowledge that this was unclear. While we measured vertical profiles (e.g. given in Appendix C, Figure C1), Figures 5 and 6 only show surface data. The following adjustments were made to captions and part of the text that refers to these figures.

Line 139 Original phrase: Vertical profiles of underwater conductivity (Figs. 5 and 6a), conservative temperature (Fig. 6b) and depth (CTD) were measured at each site by deploying and immediately recovering using two RBR sensors: a Maestro model (depth rating of 100 m) during Leg 1, and a Concerto model (depth rating of 50 m) during Legs 2, 3 and 4.

Line 139 New phrase: Vertical profiles of underwater conductivity (**e.g. Appendix C, Figure C1**) (~~Figs. 5 and 6a~~), conservative temperature (~~Fig. 6b~~) and depth (CTD) were measured at each site by deploying and immediately recovering using two RBR sensors: a Maestro model (depth rating of 100 m) during Leg 1, and a Concerto model (depth rating of 50 m) during Legs 2, 3 and 4. **Both figures 5 and 6 only show surface data collected between 0.30 and 1.66m for underwater conductivity (Figs. 5 and 6a), and conservative temperature (Fig. 6b).**

The caption of Figure 5 was modified (in bold) to: “Figure 5. Spatial distribution of the CTD-measured **surface** salinity (conductivity) during the four WP4 Nunataryuk expeditions (Legs 1, 2, 3 and 4) in 2019. Note the log₁₀ color scale used to visualize the salinity gradient. **Surface here refers to samples collected between 0.30 and 1.66 m.**”

We also added a phrase (in bold) at the end of the Figure 6 Caption: “Figure 6. Boxplots showing an overview of the: (aA) salinity; (bB) water temperature; (cC) $\delta^{18}\text{O}$; as well as a set of organic matter related parameters measured during the four Legs; (dD) $a_{\text{CDOM}}(443)$ (absorption of colored dissolved organic matter measured at 443 nm); (eE) DOC (dissolved organic matter); (fF) SUVA_{350} (specific ultraviolet absorbance at 350 nm, i.e. $a_{\text{CDOM}}(350) / \text{DOC}$); (gG) SPM (suspended particulate matter); (hH) POC (particulate organic carbon); (iI) $a_p(443)$ (absorption of particulate matter measured at 443 nm). **Note that while vertical profiles were conducted, only surface samples (from 0.3 to 1.66 m) are shown in these boxplots.**”

10-Section 4.1.2: Two methods were used (Ultrapath and dual-beam spectrophotometer). First, what was the threshold used to switch from one method to the other? Second, how many samples were measured using the Ultrapath and how many with the dual-beam spectrophotometer. Please add this information in the text.

Author reply: The ultrapath method was used for ALL the data collected during the main Nunataryuk campaigns Legs 1 to 4 (sections 4.1 to 4.3, this represents ca. 150 observations). As mentioned in *section 4.4 Supplementary data*, the opportunity for additional sampling by another set of team members (see Table 2 for PI information) arose and a subset of variables were measured in two sites near Tuktoyaktuk between July 20th and August 5th 2019 for groundwater, thawed permafrost and massive ice. These samples served to conduct several analyses, including CDOM fluorescence measurements (Table 2) using dual beam spectrophotometer. In section 4.4.2 Groundwater, it is mentioned that seawater samples (for CDOM analysis among other things) were also collected in front of each study site at ~0.5, 1, 1.5, and 2 km from the coastline. There is no intention here to compare both sets of data (Main and Supplementary data) as they are unrelated temporally and spatially. A sentence was added in section 4.4.2.2 to make this clearer:

“Note, that the method used to measure CDOM and DOC for these samples differs from samples described in section 4.1.2 and 4.1.3.”

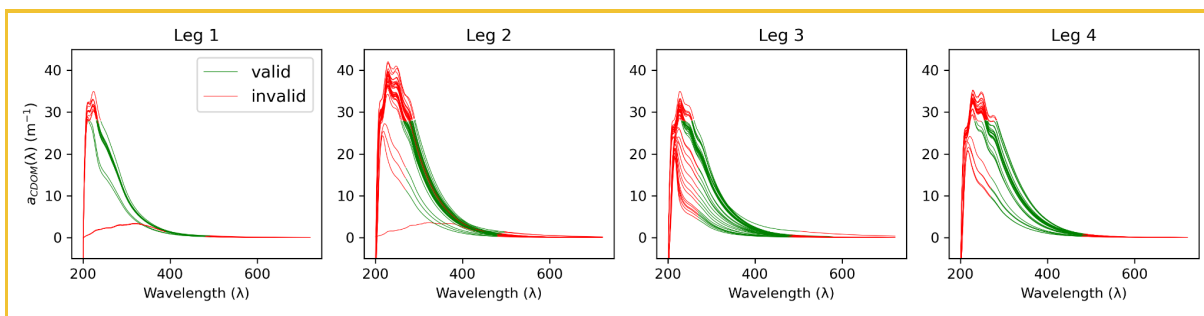
11-Also, a pathlength of 200-cm is likely to be too long for UV measurements made at 254 nm in these coastal waters and nearshore waters (and perhaps for some made at 350 nm).

Author reply. Correct. Using a 200cm optical pathlength was indeed too long for the UV range for a number of samples that showed high DOM concentrations and resulted in no or bad data. We carefully masked the data for any implausible measurements (see comment below).

12-Has there been any assessment about the quality of the CDOM absorption in the 200-300 nm range for the data measured with the Ultrathat? If there is any doubt the data are questionable below 300 nm, then it should be mentioned in the text.

Author reply: Although measurements were made for the full spectral domain (*i.e.*, 200 to 722 nm), we did not use data from 200 to 280nm due to the degradation of data quality when using the 200 cm pathlength, as pointed out by the reviewer. We modified the text to mention that data between 280 to 722 nm only was used and that a quality check was made for the rest of the shorter wavelengths (*i.e.*, 300 to 400 nm) to ensure they had not been subject to the same issue for highly absorbing waters (see masking of implausible CDOM data in figure below). The following phrases (in bold) were added to section 4.1.2. Absorption coefficients for colored dissolved organic matter:

Filtered samples were then pumped into the sample cell of an UltraPath liquid waveguide system **that included both 200 cm and 10 cm cells** (World Precision Instruments, Inc.) using a peristaltic pump, and the **absorbance** ~~absorption coefficient~~ was measured over the wavelengths ranging from 200 to 722 nm (see Bricaud et al., 2010 and further modifications in Matsuoka et al. 2012 for the complete analytical procedures). **For most samples a 10 cm cell was used. For a limited number of cases, when low signal in the spectral domain was observed (mostly waters further offshore), a 200 cm cell was used instead. Due to a complete absorption of light in the UV-range even when using the 10 cm pathlength, measurements from 200 to 280 nm were masked. To ensure quality of the rest of the data, individual spectra were carefully checked for potential saturation, following recommendations by Lefering et al. (2017). A threshold of 1.2 absorbance unit (AU) was used, and only the data lower than the AU was included in this study.** Measurements and sample processing were conducted following the protocol *Ocean Optics and Biogeochemistry* from the International Ocean Color Coordinating Group (IOCCG Protocol Series, 2018). **Uncertainty for most of the measurements was less than five percent (determined using replicate scans).**



13-Section 4.1.4: Some clarification is needed for how SUVA₃₅₀ was calculated. Was absorbance (unitless) used here or was it absorption coefficient (units of m⁻¹)? The units of SUVA₃₅₀ suggest it is absorption coefficient. This needs to be clarified. Please specify the pathlength of the optical measurement and adjust units if absorbance was actually used.

Author reply: We added the information that the “decadal absorbance” (Absorbance divided by pathlength [m⁻¹]) was used to calculate SUVA₃₅₀:

Specific ultraviolet absorbance at 350 nm (SUVA₃₅₀, m² gC⁻¹) was calculated by dividing the **decadal absorbance (absorbance/pathlength)** at 350 nm by DOC concentration (Weishaar et al., 2003).

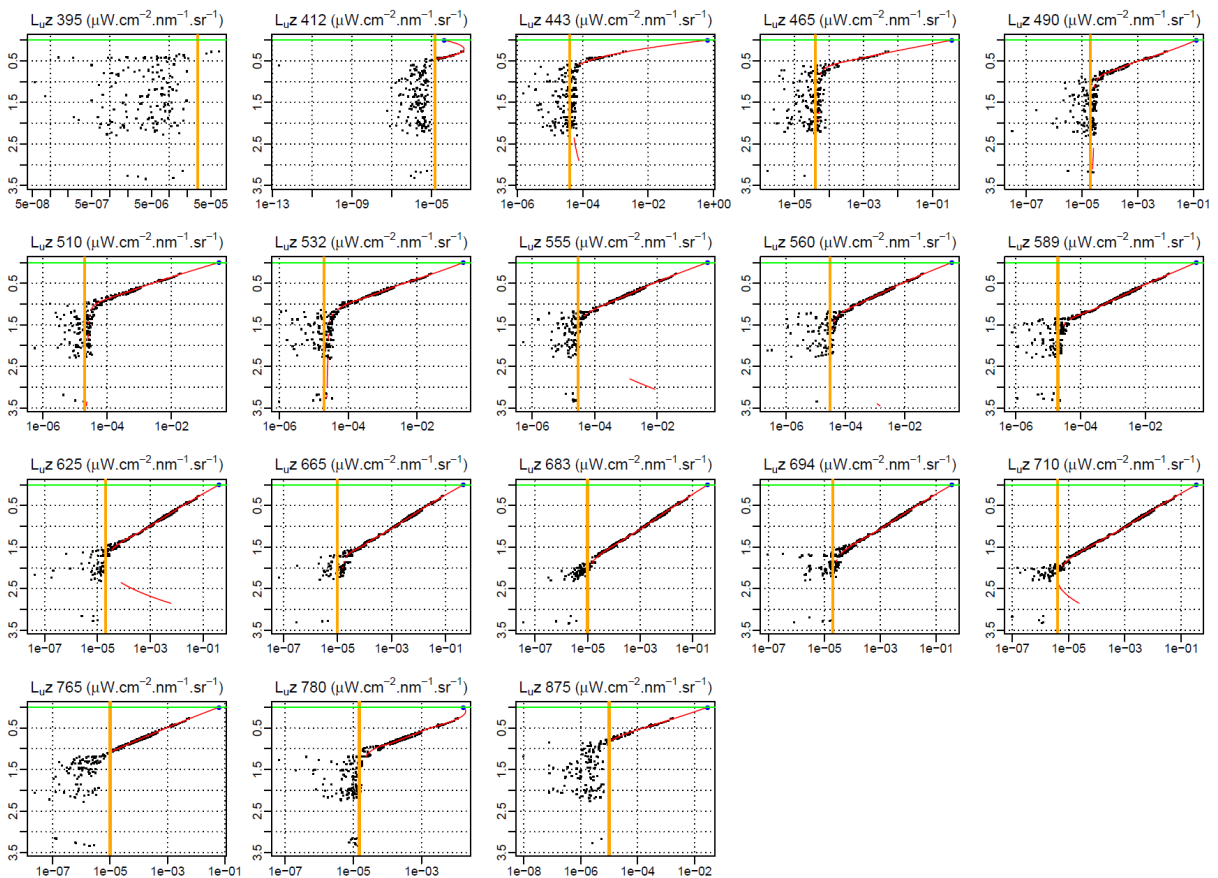
14-Sections 4.1.5 and 4.1.6: Please add references for the methods used for TCP/TCN and POC/PON. Also, provide more details regarding what standard was used for the elemental analysis, and what procedure was used to account for the blank.

Author reply: More detail was added in section 4.1.5 (see in **bold**): Due to the presence of large amounts of matter, subsections of the filters were **randomly** taken with a specialized punching tool. Two punched replicates were placed into tin capsules and processed in a Perkin Elmer elemental analyzer (PE 2400 Series-II CHNS/O Analyzer). **Acetanilide was used as a calibration standard for the CHN analysis (carbon = 71,09%, hydrogen = 6,71, nitrogen = 10,36%). Instrument blanks (empty tin capsules) are performed during calibration to stabilize and establish a baseline for the instrument.**

In addition, more detail was added in section 4.1.6. Particulate organic matter (see in **bold**): Water samples for the determination of particulate organic carbon (POC) and nitrogen (PON) **were processed according to methods described in IOCCG Protocol Series (2021). Samples were** filtered through a glass filtration unit on pre-combusted Whatman GF/F (0.7 μm) 47 mm filters with filtration volumes ranging from 250 to 1600 mL.

15-Section 4.1.8 and Figure 8: Some of the blue reflectances from Leg 4 (where $R_{rs}(412)$ are higher than $R_{rs}(443)$) are a little suspect and seem unlikely in this type of coastal waters. Consider acknowledging this issue in the text so the users are aware.

Author reply: We acknowledge here that some blue reflectance values were unlikely in these sediment-dominated and strongly absorbing waters: on three different occasions during Leg 4, $R_{rs}(412)$ were higher than $R_{rs}(443)$. The reviewer is correct in saying that higher $R_{rs}(412)$ compared to $R_{rs}(443)$ are not expected in these waters. Indeed, in such waters, the incident solar light entering the water column is more efficiently absorbed at 412 nm than at 443 nm (as the contribution to light absorption by both colored dissolved organic matter and non-algal particles increases exponentially towards short visible wavelengths, while light backscattering follows smooth (power-law) spectral variations). Therefore it is expected to obtain a R_{rs} signal decreasing from 443 to 412 nm, i.e. have $R_{rs}(412) < R_{rs}(443)$. Higher $R_{rs}(412)$ are related to the difficulty of extrapolating subsurface ($z < 0$) radiometric profiles to the surface ($z = 0$). Light at lower wavelengths is penetrating significantly less into the water column resulting in no light availability already after some centimeters, consequently leading to less data that we could use to fit and extrapolate to the surface (see Figure below). Most of these data were masked based on the quality of the fit (r^2) to the surface, however some challenges remain. This issue is discussed in more detail in Juhls et al. 2022.



The above figure shows profiles (y-axis shows depth in meter) of subsurface upwelling radiance that were used to retrieve R_{rs} at depth=0 (green line) for a selected station. Light at

low wavelength is quickly absorbed by the high absorption by organic matter. This results in no possible fitting of the data or lower quality of the fit (lower r^2 ; red line).

Another reason for these unexpected results can be related to an over-correction of the IcePro self-shadow effects enhanced by high absorption at short visible wavelengths (here 412 nm). The slight increase of R_{rs} from 443 to 412 nm certainly highlights the fact that conditions were at the limit (high self-shadow, low signal measured) of the method developed to accurately correct for self-shadow effects. Users should be aware that in the most turbid stations sampled, uncertainties associated to R_{rs} values increase towards short visible wavelengths

Author reply. The following phrase in bold was added to the text at the end of section 4.1.8 Radiometric data

Figure 8 shows the remote sensing reflectance determined following procedures by Antoine et al. (2013) and Bélanger et al. (2017). The highest values of reflectance are present between 550 and 700 nm (green to red) and the spectra show a strong influence of CDOM absorbing light in the shorter spectral domain. This set of remote sensing reflectance measurements can be useful to test and develop algorithms for retrieving water constituents using optical remote sensing and to evaluate the performance of atmospheric correction algorithms. **Note, that the retrieval of R_{rs} from profiling downwelling irradiance (E_d) and upwelling radiance (L_u) measurements in optically complex waters is extremely challenging (see also Juhls et al. 2022). The strong absorption by organic matter in low wavelengths can result in higher uncertainties of the R_{rs} . This might explain the unexpected higher $R_{rs}(412)$ compared to $R_{rs}(443)$ for a few spectra.**

16-Section 4.1.9: The title is misleading and this section is quite incomplete. It needs to be completed. The data here are actually backscattering coefficients and particle size distributions, though this is never mentioned in the text. The term Inherent Optical Properties used in the title is a broader term that includes other variables presented earlier in the manuscript (like absorption coefficient). Please adjust the title and describe what variables were produced here. Also, there needs to be referencing the methodology used to process the Hydroscat, BB3, and LISST data, and some brief description of the methods.

Author reply: We agree with the reviewer that this section is incomplete. To be honest we had hoped to have the data completely analyzed and cleaned before the end of the review process, but unfortunately that was not possible. We modified the title of this subsection and reworded the text to only keep basic information on what sensors were deployed, when, and what they allow to retrieve.

The following section was modified as such:

4.1.9 Inherent optical properties

To measure inherent optical properties (IOP) in the water column, an optical package was deployed during all four legs of the expedition. During Leg 1, the optical package included a very sensitive depth sensor (RBR model Virtuoso, accurate to 0.01 m), a particle size distribution and concentration meter (Sequoia Scientific, model LISST-100x, sensitive to 0.1 mg L^{-1}), as well as a data logger (Seabird Scientific, model DH4), all fitted in a cylindrical metallic frame that was manually lowered through an auger hole in the ice using a tripod and a hoisting system. During Legs 2, 3 and 4, the optical package included a different secondary CTD (RBR Concerto, see section 4.1 for its specifications), the same particle size distribution and concentration meter and data logger, 2 back-scattering meters (a HydroScat-2 from HobiLabs, accurate to 1×10^{-4} to $1 \times 10^5 \text{ m}^{-1}$) and a BB3 from Seabird Scientific, accurate to 0.003 m^{-1}), and a fluorescence meter (model FLBBGD from Seabird Scientific, accurate to $0.015 \text{ } \mu\text{g L}^{-1}$ for the chlorophyll-a pigment and to 0.28 ppb for the CDOM). All the sensors were factory calibrated prior to the expedition. The cylindrical frame was lowered at sea using a drill-operated winch during helicopter hovering flights, or using a motorized pulley with a davit when sampling from small fishing boats. In both cases, an electro-mechanical cable allowed for real-time data acquisition and minimal quality control. The instrumentation descent rate was very slow (ca. $0.05\text{-}0.20 \text{ m s}^{-1}$) to allow for a maximal resolution of the strong vertical gradients characteristic of several of the stations sampled. See Table 2 for details on availability of data.

4.1.9. Other optical parameters

A so-called optical frame was also deployed during the boat sampling of the Legs 2, 3 and 4. This frame was equipped with: a BB3 from SeaBird Scientific, a FLBBGD from Seabird Scientific, a HydroScat-2 from HobiLabs, an AC-9 (with a 10 cm pathlength) from SeaBird Scientific, as well as a LISST-100X (sometimes fitted with a path reduction module, in very turbid waters) from Sequoia Scientific. These sensors allow to retrieve profiles of the backscattering coefficients at six wavelengths, the concentration of Chl-a and of CDOM, the absorption coefficients at nine wavelengths, the beam attenuation at nine wavelengths, as well as particle volume and size distribution between 1.25 and 250 microns. These data have not yet been fully processed and will be published at a later time (see Appendix D for further information on the processing of light absorption (a) and scattering (b) coefficients).

Mention of the “IOP” data was also modified in Table 2, by changing the title of the table subsection ~~Inherent Optical Properties~~ to **“Other optical parameters”** and deleting the following lines (variables) from the Table:

particulate backscattering (bbp) at 550 nm
particulate backscattering (bbp) at 700 nm
particulate backscattering (bbp) at 720 nm
particulate backscattering (bbp) at 770 nm
particulate backscattering (bbp) at 850 nm

particulate backscattering (bbp) at 870 nm
concentration of Chl-a
concentration of CDOM
particle size distribution, between 1.25 and 250 microns
absorption coefficient (a) at 440 nm
absorption coefficient (a) at 555 nm
absorption coefficient (a) at 630 nm
absorption coefficient (a) at 715 nm
absorption coefficient (a) at 730 nm
absorption coefficient (a) at 750 nm
absorption coefficient (a) at 767 nm
absorption coefficient (a) at 820 nm
absorption coefficient (a) at 870 nm
beam attenuation coefficient (c) at 440 nm
beam attenuation coefficient (c) at 555 nm
beam attenuation coefficient (c) at 630 nm
beam attenuation coefficient (c) at 715 nm
beam attenuation coefficient (c) at 730 nm
beam attenuation coefficient (c) at 750 nm
beam attenuation coefficient (c) at 767 nm
beam attenuation coefficient (c) at 820 nm
beam attenuation coefficient (c) at 870 nm

17-Section 4.4.1: I think photo of the setup (tripod + corer), if available, would be welcome here and would help illustrate the approach. More citations for the methodology also need to be provided in the text.

Author reply: A picture of the setup of the tripod and the corer was added to the Appendix section as Figure E1 to give a visual aid. In terms of methodology, the practices to deploy the tripod and corer are not associated with any specific citations, it is simply to open the tripod, fix the corer on the cable and deploy it through a hole in the ice. We feel here that the text describes fairly well the methods used to deploy the corer using the tripod.



Figure E1. Picture taken during Leg 1 of the Nunataryuk expeditions showing the setup of the tripod and corer (Picture by Martine Lizotte).

18-Section 4.4.2.2: Please explain briefly how the EEM data were processed (and add reference).

Author reply: The text was modified to better explain how the EEM data were processed and some references were added (new text in bold):

Therefore, no Fe effect correction was applied to the DOM concentration, absorbance, and fluorescence. **The collected data were then described as excitation-emission matrices (EEMs) and different absorbance and fluorescence metrics were calculated (Fig. 13). Briefly, EEM and fluorescent metrics were produced using the eemR package proposed by Massicotte (2019) for RStudio software. Prior to extraction of the fluorescent DOM metrics, a Raman calibration was performed for each EMM to remove the dependence of the fluorescence intensities on the measurement equipment, as proposed by Lawaetz and Stedmon (2009).** ~~The biological index (BIX), humification index (HIX) and fluorescence index (FI) were extracted to trace the diagnostic state of the FDOM pool. The collected data were then described as excitation-emission matrices (EEMs) and different absorbance and fluorescence metrics were calculated (Fig. 13).~~

19-Line 495: I recommend changing “Fluorescence spectroscopy was successfully used to determine the origin of the DOM pool. Fluorescence...” by “Fluorescence spectroscopy can be indicative of the origin of the DOM pool. In this dataset, fluorescence...”...considering no analysis or comparison to other indicators were provided

Author reply: The suggested modifications were brought as follows:

Original phrase: Fluorescence spectroscopy was successfully used to determine the origin of the DOM pool. Fluorescence occurring at low excitation/emission wavelengths was associated to protein-like material originating from autochthonous production, whereas fluorescence happening at higher wavelengths was associated to humic-like material of higher molecular weight derived from terrestrial sources (Coble, 1996; Murphy et al., 2008).

New phrase: Fluorescence spectroscopy can be indicative of the origin of the DOM pool. In this dataset, fluorescence occurring at low excitation/emission wavelengths was associated to protein-like material originating from autochthonous production, whereas fluorescence happening at higher wavelengths was associated to humic-like material of higher molecular weight derived from terrestrial sources (Coble, 1996; Murphy, 2008).

Technical Corrections:

20-Abstract Lines 4-6 and again Lines 30-32: Lots of commas and convoluted sentence. I recommend rewriting for clarity.

Author reply: The following modifications were brought to lines 4-6:

Original phrase: While this process is ongoing, well-established, and its rate is accelerating, the fate of the newly-mobilized organic matter, as it transits from the watershed through the delta and into the marine system, remains poorly understood.

New phrase: While this process is ongoing and its rate is accelerating, the fate of the newly-mobilized organic matter as it transits from the watershed through the delta and into the marine system remains poorly understood.

The following modifications were brought to lines 30-32:

Original phrase: While permafrost thaw is ongoing, well-established, and its rate is accelerating (Camill, 2005; Biskaborn et al., 2019), the fate of the newly-mobilized OMT, as it transits from watersheds, to rivers and at the subsurface, into coastal waters of the Arctic Ocean remains poorly understood.

New phrase: While permafrost thaw is ongoing and its rate is accelerating (Camill, 2005; Biskaborn et al., 2019), the fate of the newly-mobilized OMT as it transits from watersheds to rivers and into coastal waters of the Arctic Ocean remains poorly understood.

Line 24: change land-mass to landmass

Author reply: The word “land-mass” was changed to “landmass”:

Major components of the Arctic cryosphere are currently exposed to acute changes due to accelerated climate warming rates at high latitude (IPCC, 2018; 2019; AMAP, 2021). In the Northern Hemisphere, nearly a quarter of the landmass ~~land-mass~~ is influenced by permafrost, perennially cryotic ground (Brown et al., 1998; Gruber, 2012; Obu et al., 2019).

Line 33: Unclear what “circulating” means here.

Author reply: The word “circulating” was not absolutely necessary to the phrase and was simply deleted for greater clarity.

Line 39 change “modifications in the productivity of the primary producers” by “change in primary production”

Author reply: The words “modifications in the productivity of the primary producers” was replaced by “change in primary production”

Gaining greater insight into these processes is crucial as they may lead, among other things, to enhanced emissions of CO₂ or other greenhouse gasses (Semiletov et al., 2013; Vonk et al., 2012; Vonk and Gustafsson, 2013; Tanski et al., 2019) and change in primary production ~~modifications in the productivity of the primary producers~~ (Kipp et al., 2018) that sustain the marine arctic food web, with unknown impacts on the communities that rely on these food sources (Fritz et al., 2017).

Line 90: remove “were sampled within this period”, it’s evident

Author reply: The words “were sampled within this period were removed:

Four field sampling periods were targeted: 1) Leg 1 took place from 17 April to 3 May 2019 (22 stations ~~were sampled within this period~~, see Fig. 2; see section 4.4.1 for details on sediment sampling); 2) Leg 2 extended from 14 June to 4 July 2019 (40 stations ~~sampled~~, Fig. 2); 3) Leg 3 took place from 25 July to 8 August 2019 (45 stations ~~sampled~~, Fig. 2; see section 4.4.2 for details on the parallel groundwater field survey); 4) Leg 4 was conducted from 26 August to 9 September 2019 (39 stations ~~sampled~~, Fig. 2; see section 4.4.1 for details on sediment sampling).

Lines 92-93: remove “sampled”

Author reply: The word “sampled” was deleted from three different places in the phrase:

Four field sampling periods were targeted: 1) Leg 1 took place from 17 April to 3 May 2019 (22 stations were sampled within this period, see Fig. 2; see section 4.4.1 for details on sediment sampling); 2) Leg 2 extended from 14 June to 4 July 2019 (40 stations ~~sampled~~, Fig. 2); 3) Leg 3 took place from 25 July to 8 August 2019 (45 stations ~~sampled~~, Fig. 2; see section 4.4.2 for details on the parallel groundwater field survey); 4) Leg 4 was conducted from 26 August to 9 September 2019 (39 stations ~~sampled~~, Fig. 2; see section 4.4.1 for details on sediment sampling).

Line 504: Change to “Water Samples”

Author reply: “Water sample” was changed to “Water samples”

Line 521: Change “Processes” to “properties” considering Processes are not “acquired”.

Author reply: The word “processes” was changed to “properties”.

Figure 13: the map with white and gray areas is a little bit unclear. Use blue for water body to make it more obvious

Author reply: The last bottom panel of Figure 13 was adjusted: the white and gray areas were replaced with blue to reflect the presence of water in the area.

Citation: <https://doi.org/10.5194/essd-2022-163-RC2>

OTHER CHANGES

1-Author. We noticed that both versions of the term CDOM were present in our ms: colored dissolved organic matter and chromophoric dissolved organic matter. We decided to keep only the “colored” version as this is more widely used by several scientists in the research community (e.g. IOCCG). The word chromophoric was replaced by colored in 3 different places of the ms:

Abstract: ...Water column profiles of physical and optical variables were measured *in situ*, while surface water, groundwater and sediment samples were collected and preserved for the determination of the composition and sources of OMT, including particulate and dissolved organic carbon (POC, DOC), and ~~colored chromophoric~~ colored dissolved organic matter (CDOM), as well as a suite of physical, chemical and biological variables...

4.1.2. Absorption coefficients for ~~colored chromophoric~~ colored dissolved organic matter and fluorescent dissolved organic matter

Water samples for the determination of absorption coefficients for **colored chromophoric** dissolved organic matter (a_{CDOM}) were filtered within 12h of water

2-Author. We noticed that when referring to Figure panels, we used upper case letters (e.g. Fig. 3A) when in fact letters in our figure panels were lower case. We changed all the upper case letters to lowercase in the text (e.g. ~~Fig. 3A~~ **Fig. 3a**)

3-Author. We noticed that the first submitted version of the manuscript did not contain a description of the fluorescence of dissolved organic matter (FDOM) data. We added these to section 4.1.2 (now named: “Absorption coefficients for colored dissolved organic matter and fluorescent dissolved organic matter”):

In addition to CDOM measurements, the fluorescence of dissolved organic matter was measured at the National Institute of Aquatic Resources, Technical University of Denmark, Copenhagen, Denmark. The sampling and processing of the water samples was identical to those for CDOM measurements. Fluorescence Excitation Emission Matrices (EEMs) were collected using an Aqualog® fluorescence spectrometer (HORIBA Jobin Yvon, Germany). Freshly produced Milli-Q water was used as reference. Fluorescence intensity was measured across emission wavelengths 300–600 nm (resolution 4.63 nm) at excitation wavelengths from 250 to 450 nm with 5 nm increments, and an integration time of 1 s. EEMs were corrected for inner-filter effects and for Raman and Rayleigh scattering (Murphy et al., 2013). The underlying fluorescent components of DOM in the EEMs were isolated by applying PARAFAC modeling and validated with split-half analysis using the “drEEM Toolbox” (Murphy et al., 2013). The fluorescent components derived from PARAFAC modeling were compared with PARAFAC components from other studies using the OpenFluor database (Murphy et al., 2014).